Available online at www.sciencedirect.com
SCIENCE DIRECT®
International Journal of Solids and Structures 43 (2006) 1117–1130
INTERNATIONAL JOURNAL OF SOLIDS and STRUCTURES
www.elsevier.com/locate/ijsolstr

Mechanism-based strain gradient plasticity in C^0 axisymmetric element

S. Swaddiwudhipong [a,*], K.K. Tho [a], J. Hua [a], Z.S. Liu [b]

[a] Department of Civil Engineering, National University of Singapore, Singapore 119260, Singapore
[b] Institute of High Performance Computing, 1 Science Park Road, #01-01, Singapore 117528, Singapore

Received 2 November 2004; received in revised form 25 May 2005
Available online 15 July 2005

Abstract

Non-uniform plastic deformation of materials exhibits a strong size dependence when the material and deformation length scales are of the same order at micro- and nano-metre levels. Recent progresses in testing equipment and computational facilities enhancing further the study on material characterization at these levels confirmed the size effect phenomenon. It has been shown that at this length scale, the material constitutive condition involves not only the state of strain but also the strain gradient plasticity. In this study, C^0 axisymmetric element incorporating the mechanism-based strain gradient plasticity is developed. Classical continuum plasticity approach taking into consideration Taylor dislocation model is adopted. As the length scale and strain gradient affect only the constitutive relation, it is unnecessary to introduce either additional model variables or higher order stress components. This results in the ease and convenience in the implementation. Additional computational efforts and resources required of the proposed approach as compared with conventional finite element analyses are minimal. Numerical results on indentation tests at micron and submicron levels confirm the necessity of including the mechanism-based strain gradient plasticity with appropriate inherent material length scale. It is also interesting to note that the material is hardened under Berkovich compared to conical indenters when plastic strain gradient is considered but softened otherwise.

Keywords: Constitutive relation; C^0 axisymmetric element; Simulated indentation test; Material length scale; Power law strain hardening; Strain gradient effect

* Corresponding author. Tel.: +65 68742173; fax: +65 67791635.
E-mail address: cvesomsa@nus.edu.sg (S. Swaddiwudhipong).

0020-7683/$ - see front matter © 2005 Elsevier Ltd. All rights reserved.
doi:10.1016/j.ijsolstr.2005.05.026

1. Introduction

The growing reliance on MEMS and NEMS and the improved capability of the indentation instrument have inspired numerous researchers to conduct material characterization based on indentation tests at micron and submicron levels. The rapid development in the field is also to exploit the significant gain in strength at smaller size. Experiments carried out in the past few decades demonstrated the strong size effects when the material length scale and the non-uniform plastic deformation are of the same order at micron or submicron levels. Classical continuum mechanics ceases to be valid at this range of deformation. Stelmashenko et al. (1993), Ma and Clarke (1995) and Nix (1997) have reported the strong size dependence in the indentation tests of single and polycrystalline metallic materials when the depth of indentation was at micron or submicron level. Similar phenomena have been observed by Fleck et al. (1994) in torsional experiments on copper wires of micron diameters and by Stolken and Evans (1998) and Haque and Saif (2003) in micro-bend tests.

Toupin (1962) and Mindlin (1965) have proposed a theory incorporating the strain gradients as additional parameters in describing the state of stress in constitutive condition of materials. Based on Taylor (1934) dislocation model, Fleck and Hutchinson (1993) proposed a phenomenological theory of strain gradient plasticity. The mechanism-based theory of strain gradient (MSG) plasticity was developed by Gao et al. (1999) and Huang et al. (2000) through the mesoscale constitutive laws incorporating the micro-scale plasticity based on Taylor dislocation model. Higher-order stress components and hence additional governing equations and boundary conditions are involved in the formulation process. These requirements imposed substantial complexities in the formulation and solution stages for both analytical work and numerical implementation. Several researchers such as Xia and Hutchinson (1996), Shu and Fleck (1998), Chen and Wang (2002a,b) and Chen and Yuan (2002) developed finite element procedures based on the mechanism-based higher-order strain gradient plasticity and applied the method to study various continuum problems at micron and sub-micron levels. As higher order stress components are included in the formulation, the approach involves either more degrees of freedom and/or C^1 continuous shape functions on top of additional governing equations and boundary conditions.

An alternative approach presented by Aifantis (1984) and Muhlhaus and Aifantis (1991) does not require the work conjugate of strain gradients. Acharya and Bassani (1996) proposed a constitutive relation model incorporating gradient-type non-local measures for rate-independent plasticity. The strain gradient effects are included in the constitutive equations through the instantaneous hardening moduli. Chen and Wang (2000) and Chen et al. (2004) adopted C^0 finite elements with both translational and rotational nodal displacements to simulate the thin wire torsion, micro-bend tests and micro-indentation with size effects based on the balance laws in a non-local theory which are identical to classical local theories (Eringen, 1981 and 1983). Gao and Huang (2001) proposed a Taylor-based non-local theory of plasticity to study void growth, cavitation instabilities, particle reinforced composites, micro-tension, micro-bending and micro-indentation. The main feature of this approach is that the resulting boundary value problems remain the same as in the conventional flow theories and no higher-order stress and stain are involved in the governing equations and boundary conditions.

Conventional theory of mechanism-based strain gradient (CMSG) was recently proposed by Huang et al. (2004). The theory retains the contribution of strain gradients based on Taylor hardening theory without involving the higher-order stress components. The effects of the strain gradients and material length scale are felt only in the constitutive relation rendering additional governing equations and boundary conditions irrelevant. The approach is much more appealing than the predecessors as only nodal displacement variables are included in the finite element formulation. The same concept has been adopted by Swaddiwudhipong et al. (2005a) to formulate and implement C^0 solid elements to study the bar under its own weight and Berkovich indentation simulation at nano-meter level.

2. Taylor dislocation model and constitutive relation

The constitutive relation incorporating Taylor dislocation model through the effective strain rate is briefly described in this section. Mechanism-based strain gradient plasticity has been introduced and proposed by several prominent researchers including Toupin (1962), Mindlin (1965), Fleck and Hutchinson (1993), Gao et al. (1999) and Huang et al. (2000). The latter in his recent work (Huang et al., 2004) presented the conventional theory of mechanism-based strain gradient plasticity. These works form the bases of the materials described in this section.

For small dislocation density, Taylor (1934) dislocation model can be simplified and expressed as (Ashby, 1970)

$$\tau = \alpha\mu b\sqrt{\rho_{\mathrm{T}}} = \alpha\mu b\sqrt{\rho_{\mathrm{S}} + \rho_{\mathrm{G}}} \tag{1}$$

where τ is the shear flow stress, b the magnitude of the Burgers vector, μ the shear modulus and α an empirical constant the value of which ranges from 0.2 to 0.5 depending on the material structures and characteristics. The total dislocation density, ρ_{T}, comprises the density of statistically stored dislocations (SSD), ρ_{S}, and the geometrically necessary dislocations (GND) density, ρ_{G}. The former, ρ_{S}, is trapped randomly and can be determined from the uni-axial stress–strain law while the latter, ρ_{G}, is introduced by Nye (1953) to ensure the compatibility of the non-uniform plastic deformation.

$$\rho_{\mathrm{G}} = \bar{r}\eta^{\mathrm{p}}/b \tag{2}$$

The expression for the flow stress of Taylor dislocation model can be shown to be (Huang et al., 2004)

$$\sigma_{\mathrm{f}} = \sqrt{[\sigma_{\mathrm{Y}} f(\varepsilon^{\mathrm{p}})]^2 + M^2\bar{r}\alpha^2\mu^2 b\eta^{\mathrm{p}}} = \sigma_{\mathrm{Y}}\sqrt{f^2(\varepsilon^{\mathrm{p}}) + l\eta^{\mathrm{p}}} \tag{3}$$

where $\sigma_{\mathrm{Y}} f(\varepsilon^{\mathrm{p}})$ represents the stress–plastic strain relation in uni-axial tension and M is the Taylor factor relating the tensile yield strength to the critical resolved shear strength for crystalline materials. η^{p} is the effective plastic strain gradient and l is the intrinsic material length scale in strain gradient plasticity introduced by Fleck and Hutchinson (1993) and can be expressed as

$$l = \bar{r}b\left(\frac{M\alpha\mu}{\sigma_{\mathrm{Y}}}\right)^2 = 18b\left(\frac{\alpha\mu}{\sigma_{\mathrm{Y}}}\right)^2 \tag{4}$$

for common values of $M = 3.06$ and $\bar{r} = 1.90$ as proposed by Bishop and Hill (1951) and Arsenlis and Parks (1999) respectively. The values of the material length scale, l, are in the order of microns incorporating the combined effects of shear modulus μ (elasticity), the yield stress σ_Y (plasticity) and the magnitude of Burgers vector b (dislocation).

The power law visco-plastic model (Hutchinson, 1976; Kok et al., 2002) incorporating the strain gradient effects is expressed as

$$\dot{\varepsilon}^{\mathrm{p}} = \dot{\varepsilon}\left[\frac{\sigma_{\mathrm{e}}}{\sigma_{\mathrm{f}}}\right]^m = \dot{\varepsilon}\left[\frac{\sigma_{\mathrm{e}}}{\sigma_{\mathrm{Y}}\sqrt{f^2(\varepsilon^{\mathrm{p}}) + l\eta^{\mathrm{p}}}}\right]^m \tag{5}$$

where $\dot{\varepsilon} = \sqrt{\frac{2}{3}\dot{\varepsilon}'_{ij}\dot{\varepsilon}'_{ij}}$ is the effective strain rate, m the rate-sensitivity exponent and $\dot{\varepsilon}'_{ij}$ the deviatoric strain rate. Huang et al. (2004) demonstrated that Eq. (5) is applicable to conventional power-law hardening if m is large ($m \geqslant 20$).

The strain rate, $\dot{\varepsilon}_{ij}$, comprises the elastic and plastic components such that

$$\dot{\varepsilon}_{ij} = \dot{\varepsilon}^{\mathrm{e}}_{ij} + \dot{\varepsilon}^{\mathrm{p}}_{ij} = \frac{1}{2\mu}\dot{\sigma}'_{ij} + \frac{\dot{\sigma}_{kk}}{9K}\delta_{ij} + \frac{3\dot{\varepsilon}^{\mathrm{p}}}{2\sigma_{\mathrm{e}}}\sigma'_{ij} \tag{6}$$

The elastic strain rate $\dot{\varepsilon}^{\mathrm{e}}_{ij}$ is obtained from the stress rate, $\dot{\sigma}_{ij}$, via the linear elastic relation.

$$\dot{\varepsilon}^{\mathrm{e}}_{ij} = \frac{1}{2\mu}\dot{\sigma}'_{ij} + \frac{\dot{\sigma}_{kk}}{9K}\delta_{ij} \tag{7}$$

$\dot{\sigma}'_{ij}$ is the deviatoric stress rate, K the bulk modulus of elasticity and $\sigma_{\mathrm{e}} = \sqrt{3\sigma'_{ij}\sigma'_{ij}/2}$ is the von Mises effective stress. The deviatoric strain rate can be obtained from

$$\dot{\varepsilon}'_{ij} = \dot{\varepsilon}_{ij} - \frac{1}{3}\dot{\varepsilon}_{kk}\delta_{ij} = \frac{1}{2\mu}\dot{\sigma}'_{ij} + \frac{3\dot{\varepsilon}^{\mathrm{p}}}{2\sigma_{\mathrm{e}}}\sigma'_{ij} \tag{8}$$

where $\dot{\varepsilon}_{kk} = \frac{\dot{\sigma}_{kk}}{3K}$ and δ_{ij} is the Kronecker delta tensor.

The effective plastic strain gradient is given by Gao et al. (1999)

$$\eta^{\mathrm{p}} = \sqrt{\eta^{\mathrm{p}}_{ijk}\eta^{\mathrm{p}}_{ijk}}\Big/2 \tag{9}$$

where $\eta^{\mathrm{p}}_{ijk} = \varepsilon^{\mathrm{p}}_{ik,j} + \varepsilon^{\mathrm{p}}_{jk,i} - \varepsilon^{\mathrm{p}}_{ij,k}; \varepsilon^{\mathrm{p}}_{ij} = \int \dot{\varepsilon}^{\mathrm{p}}_{ij}\mathrm{d}t$ and $\varepsilon^{\mathrm{p}}_{ij}$ is the plastic strain tensor. Details on the derivation are provided in the next section. In view of Eq. (5), Eq. (8) becomes

$$\dot{\varepsilon}'_{ij} = \frac{1}{2\mu}\dot{\sigma}'_{ij} + \frac{3\dot{\varepsilon}}{2\sigma_{\mathrm{e}}}\left(\frac{\sigma_{\mathrm{e}}}{\sigma_{\mathrm{f}}}\right)^{m}\sigma'_{ij} = \frac{1}{2\mu}\dot{\sigma}'_{ij} + \frac{3\dot{\varepsilon}}{2\sigma_{\mathrm{e}}}\left(\frac{\sigma_{\mathrm{e}}}{\sigma_{\mathrm{Y}}\sqrt{f^2(\varepsilon^{\mathrm{p}}) + l\eta^{\mathrm{p}}}}\right)^{m}\sigma'_{ij} \tag{10}$$

The stress rate can thus be expressed as

$$\dot{\sigma}_{ij} = K\dot{\varepsilon}_{kk}\delta_{ij} + 2\mu\left[\dot{\varepsilon}'_{ij} - \frac{3\dot{\varepsilon}}{2\sigma_{\mathrm{e}}}\left(\frac{\sigma_{\mathrm{e}}}{\sigma_{\mathrm{Y}}\sqrt{f^2(\varepsilon^{\mathrm{p}}) + l\eta^{\mathrm{p}}}}\right)^{m}\sigma'_{ij}\right] \tag{11}$$

Eq. (11) as mentioned by Huang et al. (2004) describes the constitutive relation considering the strain gradient effect without the presence of higher-order stress components. Conventional continuum mechanic algorithms which are readily available can be employed with minor alterations and minimal additional computational efforts and resources.

3. Effective strain gradient

3.1. Orthogonal curvilinear coordinate system

Though the effective strain gradient tensor, $\boldsymbol{\eta}$, derived in this section is based on the total strain and deformation, the relations are applicable for expressions for effective plastic strain gradient, η^{p}, required of in Eq. (5) as the elastic component is usually small and can be ignored (Fleck and Hutchinson, 1997). The strain gradient tensor of third-order, $\boldsymbol{\eta}$, is defined as

$$\boldsymbol{\eta} = \nabla\nabla\mathbf{u} \tag{12}$$

The displacement vector, $\mathbf{u}$, is expressed as

$$\mathbf{u} = \sum_i u_i\tilde{\mathbf{e}}_i \tag{13}$$

where $\tilde{\mathbf{e}}_i$ is the unit vector in i direction. The gradient, ∇, in orthogonal curvilinear coordinate system is defined as

$$\nabla(\,) = \sum_i \tilde{\mathbf{e}}_i \frac{1}{h_i}\frac{\partial(\,)}{\partial\alpha_i} \tag{14}$$

where α_i is the orthogonal curvilinear coordinate in i direction and h_i the corresponding Lamé coefficient. The derivatives of unit base vectors can be shown to be

$$\frac{\partial \tilde{\mathbf{e}}_i}{\partial \alpha_i} = -\frac{1}{h_k}\frac{\partial h_i}{\partial \alpha_k}\tilde{\mathbf{e}}_k - \frac{1}{h_j}\frac{\partial h_i}{\partial \alpha_j}\tilde{\mathbf{e}}_j, \quad \frac{\partial \tilde{\mathbf{e}}_i}{\partial \alpha_j} = \frac{1}{h_i}\frac{\partial h_j}{\partial \alpha_i}\tilde{\mathbf{e}}_j \tag{15}$$

where i, j, k are unequal mutually. The strain gradient tensor in orthogonal curvilinear coordinate system can thus be expressed as

$$\begin{aligned}
\boldsymbol{\eta} &= \nabla\nabla\mathbf{u} = \nabla\nabla\left(\sum_i u_i\tilde{\mathbf{e}}_i\right) = \nabla\left[\sum_j \tilde{\mathbf{e}}_j \frac{1}{h_j}\frac{\partial}{\partial \alpha_j}\left(\sum_i u_i\tilde{\mathbf{e}}_i\right)\right] \\
&= \sum_{i,j,k}\frac{1}{h_j h_k}\left(\frac{\partial^2 u_i}{\partial\alpha_j\partial\alpha_k}\tilde{\mathbf{e}}_k\tilde{\mathbf{e}}_j\tilde{\mathbf{e}}_i + \frac{\partial u_i}{\partial\alpha_j}\tilde{\mathbf{e}}_k\frac{\partial\tilde{\mathbf{e}}_j}{\partial\alpha_k}\tilde{\mathbf{e}}_i + \frac{\partial u_i}{\partial\alpha_j}\tilde{\mathbf{e}}_k\tilde{\mathbf{e}}_j\frac{\partial\tilde{\mathbf{e}}_i}{\partial\alpha_k}\right) \\
&\quad + \sum_{i,j,k}\frac{1}{h_j h_k}\left(\frac{\partial u_i}{\partial\alpha_k}\tilde{\mathbf{e}}_k\tilde{\mathbf{e}}_j\frac{\partial\tilde{\mathbf{e}}_i}{\partial\alpha_j} + u_i\tilde{\mathbf{e}}_k\frac{\partial\tilde{\mathbf{e}}_j}{\partial\alpha_k}\frac{\partial\tilde{\mathbf{e}}_i}{\partial\alpha_j} + u_i\tilde{\mathbf{e}}_k\tilde{\mathbf{e}}_j\frac{\partial^2\tilde{\mathbf{e}}_i}{\partial\alpha_j\partial\alpha_k}\right) \\
&\quad + \sum_{i,j,k}\left(\frac{1}{h_k}\frac{\partial}{\partial\alpha_k}\left(\frac{1}{h_j}\right)\frac{\partial u_i}{\partial\alpha_j}\tilde{\mathbf{e}}_k\tilde{\mathbf{e}}_j\tilde{\mathbf{e}}_i + \frac{1}{h_k}\frac{\partial}{\partial\alpha_k}\left(\frac{1}{h_j}\right)u_i\tilde{\mathbf{e}}_k\tilde{\mathbf{e}}_j\frac{\partial\tilde{\mathbf{e}}_i}{\partial\alpha_j}\right) \\
&= a1 + a2 + a3 + a4 + a5 + a6 + a7 + a8
\end{aligned} \tag{16}$$

3.2. Cylindrical coordinates and axisymmetric element

The corresponding coordinates, unit vectors, their first and second derivatives and Lamé coefficients in cylindrical coordinate system can be expressed respectively as

$$\alpha_1 = r, \quad \alpha_2 = \theta, \quad \alpha_3 = z \tag{17}$$

$$\tilde{\mathbf{e}}_1 = \mathbf{e}_r, \quad \tilde{\mathbf{e}}_2 = \mathbf{e}_\theta, \quad \tilde{\mathbf{e}}_3 = \mathbf{e}_z \tag{18}$$

$$\frac{\partial\mathbf{e}_\theta}{\partial\theta} = -\frac{1}{h_r}\frac{\partial h_\theta}{\partial r}\mathbf{e}_r - \frac{1}{h_z}\frac{\partial h_\theta}{\partial z}\mathbf{e}_z = -\frac{1}{h_r}\mathbf{e}_r = -\mathbf{e}_r \tag{19}$$

$$\frac{\partial\mathbf{e}_r}{\partial\theta} = \frac{1}{h_r}\frac{\partial h_\theta}{\partial r}\mathbf{e}_\theta = \frac{1}{h_r}\frac{\partial h_\theta}{\partial r}\mathbf{e}_\theta = \mathbf{e}_\theta \tag{20}$$

$$\frac{\partial^2\mathbf{e}_\theta}{\partial\theta^2} = -\frac{\partial\mathbf{e}_r}{\partial\theta} = -\mathbf{e}_\theta, \quad \frac{\partial^2\mathbf{e}_r}{\partial\theta^2} = -\frac{\partial\mathbf{e}_\theta}{\partial\theta} = -\mathbf{e}_r \tag{21}$$

$$h_r = 1, \quad h_\theta = r, \quad h_z = 1 \tag{22}$$

The following relations are valid for axisymmetric case:

$$u_\theta = 0 \quad \text{and} \quad \frac{\partial u_r}{\partial\theta} = \frac{\partial u_z}{\partial\theta} = 0 \tag{23}$$

Considering Eqs. (17)–(22), if axisymmetric conditions are imposed in Eq. (16) the eight components of the strain gradient are further simplified to

$$a1 = \sum_{i,j,k=r,z} u_{i,jk}\mathbf{e}_j\mathbf{e}_k\mathbf{e}_i \tag{24}$$

$$a2 = \frac{1}{r}\sum_{i=r,z} u_{i,r}\mathbf{e}_\theta\mathbf{e}_\theta\mathbf{e}_i \tag{25}$$

$$a3 = \frac{1}{r}\sum_{i=r,z} u_{r,i}\mathbf{e}_\theta\mathbf{e}_i\mathbf{e}_\theta \tag{26}$$

$$a4 = \frac{1}{r}\sum_{i=r,z} u_{r,i}\mathbf{e}_i\mathbf{e}_\theta\mathbf{e}_\theta \tag{27}$$

$$a5 = -\frac{u_r}{r^2}\mathbf{e}_\theta\mathbf{e}_r\mathbf{e}_\theta \tag{28}$$

$$a6 = -\frac{u_r}{r^2}\mathbf{e}_\theta\mathbf{e}_\theta\mathbf{e}_r \tag{29}$$

$$a7 = 0 \tag{30}$$

$$a8 = -\frac{u_r}{r^2}\mathbf{e}_r\mathbf{e}_\theta\mathbf{e}_\theta \tag{31}$$

The strain gradient tensor for axisymmetric element, $\boldsymbol{\eta}$, can thus be expressed as

$$\begin{aligned}\boldsymbol{\eta} = \nabla\nabla\mathbf{u} &= a1 + a2 + a3 + a4 + a5 + a6 + a7 + a8 \\ &= \sum_{i,j,k=r,z} u_{i,jk}\mathbf{e}_j\mathbf{e}_k\mathbf{e}_i + \frac{1}{r}\sum_{i=r,z}\left(u_{i,r}\mathbf{e}_\theta\mathbf{e}_\theta\mathbf{e}_i + u_{r,i}\mathbf{e}_\theta\mathbf{e}_i\mathbf{e}_\theta + u_{r,i}\mathbf{e}_i\mathbf{e}_\theta\mathbf{e}_\theta\right) - \frac{u_r}{r^2}\left(\mathbf{e}_\theta\mathbf{e}_r\mathbf{e}_\theta + \mathbf{e}_\theta\mathbf{e}_\theta\mathbf{e}_r + \mathbf{e}_r\mathbf{e}_\theta\mathbf{e}_\theta\right)\end{aligned} \tag{32}$$

The relations of strain gradient components are thus

$$\eta_{rrr} = u_{r,rr} \quad \eta_{rrz} = u_{z,rr} \tag{33}$$

$$\eta_{zzr} = u_{r,zz} \quad \eta_{zzz} = u_{z,zz} \tag{34}$$

$$\eta_{rzr} = \eta_{zrr} = u_{r,rz} \quad \eta_{rzz} = \eta_{zrz} = u_{z,rz} \tag{35}$$

$$\eta_{\theta z\theta} = \eta_{z\theta\theta} = \frac{1}{r}u_{r,z} \quad \eta_{\theta\theta z} = \frac{1}{r}\frac{\partial u_z}{\partial r} \tag{36}$$

$$\eta_{r\theta\theta} = \eta_{\theta r\theta} = \eta_{\theta\theta r} = \frac{1}{r}u_{r,r} - \frac{u_r}{r^2} \tag{37}$$

The deviatoric strain gradient tensor is defined as

$$\eta'_{ijk} = \eta_{ijk} - \frac{1}{4}\left(\delta_{ik}\eta_{jpp} + \delta_{jk}\eta_{ipp}\right) \tag{38}$$

Hence the components of deviatoric strain gradient can be shown to be

$$\eta'_{rrr} = \frac{1}{2}\eta_{rrr} - \frac{1}{2}(\eta_{r\theta\theta} + \eta_{rzz}) = \frac{1}{2}u_{r,rr} - \frac{1}{2}\left(\left(\frac{1}{r}u_{r,r} - \frac{u_r}{r^2}\right) + u_{z,zr}\right) \tag{39}$$

$$\eta'_{rrz} = \eta_{rrz} = u_{z,rr} \quad \eta'_{zzr} = \eta_{zzr} = u_{r,zz} \tag{40}$$

$$\eta'_{r\theta\theta} = \eta'_{\theta r\theta} = \frac{3}{4}\eta_{r\theta\theta} - \frac{1}{4}(\eta_{rrr} + \eta_{rzz}) = \frac{3}{4}\left(\frac{1}{r}u_{r,r} - \frac{u_r}{r^2}\right) - \frac{1}{4}(u_{r,rr} + u_{z,zr}) \tag{41}$$

$$\eta'_{rzr} = \eta'_{zrr} = \frac{3}{4}\eta_{rzr} - \frac{1}{4}(\eta_{z\theta\theta} + \eta_{zzz}) = \frac{3}{4}u_{r,zr} - \frac{1}{4}\left(\frac{1}{r}u_{r,z} + u_{z,zz}\right) \tag{42}$$

$$\eta'_{rzz} = \eta'_{zrz} = \frac{3}{4}\eta_{rzz} - \frac{1}{4}(\eta_{rrr} + \eta_{r\theta\theta}) = \frac{3}{4}u_{z,zr} - \frac{1}{4}\left(u_{r,rr} + \left(\frac{1}{r}u_{r,r} - \frac{u_r}{r^2}\right)\right) \tag{43}$$

$$\eta'_{\theta\theta r} = \eta_{\theta\theta r} = \frac{1}{r}u_{r,r} - \frac{u_r}{r^2} \quad \eta'_{\theta\theta z} = \eta_{\theta\theta z} = \frac{1}{r}u_{z,r} \tag{44}$$

$$\eta'_{\theta z\theta} = \eta'_{z\theta\theta} = \frac{3}{4}\eta_{\theta z\theta} - \frac{1}{4}(\eta_{zrr} + \eta_{zzz}) = \frac{3}{4}\frac{1}{r}u_{r,z} - \frac{1}{4}(u_{r,rz} + u_{z,zz}) \tag{45}$$

$$\eta'_{zzz} = \frac{1}{2}\eta_{zzz} - \frac{1}{2}(\eta_{zrr} + \eta_{z\theta\theta}) = \frac{1}{2}u_{z,zz} - \frac{1}{2}\left(u_{r,rz} + \frac{1}{r}u_{r,z}\right) \tag{46}$$

4. C^0 axisymmetric element for materials with stain gradient effects

Finite element analyses have been adopted to study complex elastic, elasto-plastic, visco-elastic and visco-plastic problems. During the early part of the past decade, the method without strain gradient effects has been used to simulate Berkovich and other pyramidal indentation tests such as those presented by Larsson et al. (1996), Giannakopoulos and Larsson (1997) and Swaddiwudhipong et al. (2005b). Several researchers notably Fleck, Hutchinson and their co-workers in the later part of the previous decade have developed finite elements incorporating strain gradient plasticity effects based on higher-order continuum plasticity theory. A few examples are those reported by Xia and Hutchinson (1996), Begley and Hutchinson (1998), Shu and Fleck (1998), Shu et al. (1999) and Chen and Yuan (2002). Either C^1-continuous shape functions or additional degrees of freedom have to be adopted in their works. The formulation of finite element equations and the imposition of boundary conditions are awkward and tedious. In this paper, C^0 axisymmetric element incorporating conventional mechanism-based strain gradient plasticity is formulated, implemented and adopted in the study of simulated indentation tests. An eight-node isoparametric element is adopted as an example demonstrating the formulation of governing finite element equations. Its counterpart ignoring the strain gradient effects has been widely used and available in most commercial finite element programs.

Let r, z and u, w be the coordinates and displacement components in the radial direction and along the axisymmetric axis, respectively. They can be expressed through isoparametric concept for an eight-node axisymmetric element as

$$r = \sum_{i=1}^{8} N_i(g,h) r_i, \quad z = \sum_{i=1}^{8} N_i(g,h) z_i \tag{47}$$

$$u = \sum_{i=1}^{8} N_i(g,h) u_i, \quad w = \sum_{i=1}^{8} N_i(g,h) w_i \tag{48}$$

where g and h are the corresponding natural coordinates. The shape functions, N_i ($i = 1$–8) are well known and can be obtained in any finite element texts, e.g., Zienkiewicz and Taylor (1994). Coordinate transformation can be performed through Jacobian matrix and its inverse expressed as

$$J = \frac{\partial(r,z)}{\partial(g,h)} = \begin{bmatrix} r_{,g} & r_{,h} \\ z_{,g} & z_{,h} \end{bmatrix} \tag{49}$$

$$J^{-1} = \frac{\partial(g,h)}{\partial(r,z)} = \begin{bmatrix} g_{,r} & g_{,z} \\ h_{,r} & h_{,z} \end{bmatrix} \tag{50}$$

The strain vector $\{\varepsilon\}$ can be expressed as

$$\{\varepsilon\} = \left[\frac{\partial u}{\partial r} \quad \frac{u}{r} \quad \frac{\partial w}{\partial z} \quad \frac{\partial u}{\partial z} + \frac{\partial w}{\partial r}\right]^{\mathrm{T}} = [B]\{\delta\} \tag{51}$$

$$[B] = [\,B_1 \quad B_2 \quad \cdots \quad B_8\,] \tag{52}$$

$$\{\delta\} = [\,\delta_1 \quad \delta_2 \quad \cdots \quad \delta_8\,] \tag{53}$$

$$[B_i] = \begin{bmatrix} N_{i,r} & 0 \\ \dfrac{N_i}{r} & 0 \\ 0 & N_{i,z} \\ N_{i,z} & N_{i,r} \end{bmatrix}, \quad \{\delta_i\} = \begin{Bmatrix} u_i \\ w_i \end{Bmatrix}, \quad i = 1\text{–}8 \tag{54}$$

Coordinate transformation can be carried out through Eq. (55).

$$[N_{i,r} \quad N_{i,z}] = [N_{i,g} \quad N_{i,h}]J^{-1} \tag{55}$$

The strain gradients can be obtained through the derivation of the strain vector shown in Eqs. (51)–(54).

$$\{\varepsilon\}_{,r} = \left[\frac{\partial^2 u}{\partial r^2} \ \frac{1}{r}\frac{\partial u}{\partial r} - \frac{u}{r^2} \ \frac{\partial^2 w}{\partial r \partial z} \ \frac{\partial^2 u}{\partial z \partial r} + \frac{\partial^2 w}{\partial r^2}\right]^{\mathrm{T}} = [B]_{,r}\{\delta\} \tag{56}$$

$$[B_i]_{,r} = \begin{bmatrix} N_{i,rr} & 0 \\ \frac{1}{r}N_{i,r} - \dfrac{N_i}{r^2} & 0 \\ 0 & N_{i,zr} \\ N_{i,zr} & N_{i,rr} \end{bmatrix} \tag{57}$$

The derivatives of strain vector with respect to z can be similarly derived. According to the chain rule,

$$N_{i,rr} = \frac{\partial N_{i,r}}{\partial g}\frac{\partial g}{\partial r} + \frac{\partial N_{i,r}}{\partial h}\frac{\partial h}{\partial r} = N_{i,rg}g_{,r} + N_{i,rh}h_{,r} \tag{58}$$

Hence,

$$\begin{bmatrix} N_{i,rr} & N_{i,rz} \\ N_{i,zr} & N_{i,zz} \end{bmatrix} = \begin{bmatrix} N_{i,rg} & N_{i,rh} \\ N_{i,zg} & N_{i,zh} \end{bmatrix} \begin{bmatrix} g_{,r} & g_{,z} \\ h_{,r} & h_{,z} \end{bmatrix} \tag{59}$$

Eq. (59) can be expressed in compact form as

$$\frac{\partial(N_{i,r}, N_{i,z})}{\partial(r,z)} = \frac{\partial(N_{i,r}, N_{i,z})}{\partial(g,h)}\frac{\partial(g,h)}{\partial(r,z)} = \frac{\partial(N_{i,r}, N_{i,z})}{\partial(g,h)}J^{-1} \tag{60}$$

Similarly,

$$N_{i,gg} = N_{i,gr}r_{,g} + N_{i,gz}z_{,g} \tag{61}$$

$$\frac{\partial(N_{i,g}, N_{i,h})}{\partial(g,h)} = \frac{\partial(N_{i,g}, N_{i,h})}{\partial(r,z)}\frac{\partial(r,z)}{\partial(g,h)} = \frac{\partial(N_{i,g}, N_{i,h})}{\partial(r,z)}J \tag{62}$$

Note that

$$\frac{\partial(N_{i,r}, N_{i,z})}{\partial(g,h)} = \left(\frac{\partial(N_{i,g}, N_{i,h})}{\partial(r,z)}\right)^{\mathrm{T}} \tag{63}$$

It can be shown that

$$\frac{\partial(N_{i,r}, N_{i,z})}{\partial(r,z)} = J^{-T}\frac{\partial(N_{i,g}, N_{i,h})}{\partial(g,h)}J^{-1} \tag{64}$$

The strain and the strain gradient matrices have been derived based on the above concept and the expressions implemented in the user subroutine of the finite element package ABAQUS (2002).

5. Numerical examples

5.1. Simulated indentation on nickel

Various finite element analyses have been carried out to simulate the indentation tests at submicron level reported earlier. Both conventional elements and those incorporating mechanism-based strain gradient effects presented in this paper are employed to simulate the load–displacement relationship of Berkovich indentation on electro-polished nickel conducted by Pethica et al. (1983). The material properties as adopted earlier by Bhattacharya and Nix (1988) to simulate this test are employed in the study. They are as follows: the Young's modulus of elasticity, $E = 207$ GPa, the yield strength, $Y = 350$ MPa, the power law, $n = 0.03$ and the Poisson's ratio, $v = 0.33$. The intrinsic material length scale for Nickel of 5 μm stipulated by Wang et al. (2003) is adopted in the analyses.

The convergence study of axisymmetric element meshes with and without the effects of strain gradient for the equivalent conical indentation with a half angle of 70.3° has been carried out. The indenter is idealized as a rigid body in the finite element model while the target material (nickel) is modeled as a deformable body. Three different meshes employing 5736, 10,107 and 15,816 axisymmetric elements for the target domain have been employed in the study. A typical finite element mesh for the latter is shown in Fig. 1. In each mesh, a uniform fine mesh is adopted in the region of 2×2 μm in the vicinity of the contact domain where high stress concentration is expected. The size of each element in this region for the finest mesh is 20×20 nm with an aspect ratio of one. The element size is gradually increased further away from this region. The average aspect ratio of the elements is kept closed to one throughout the whole domain. Frictionless contact is assumed in the present finite element simulation, as its effect is negligible for indenters with half-angle larger than 60° as reported by Bucaille et al. (2003). The convergence of the results obtained from the three meshes can be observed through the graph depicted in Fig. 2. Though the results from the coarser mesh are observed to converge satisfactorily, the finest mesh has been adopted in other analyses.

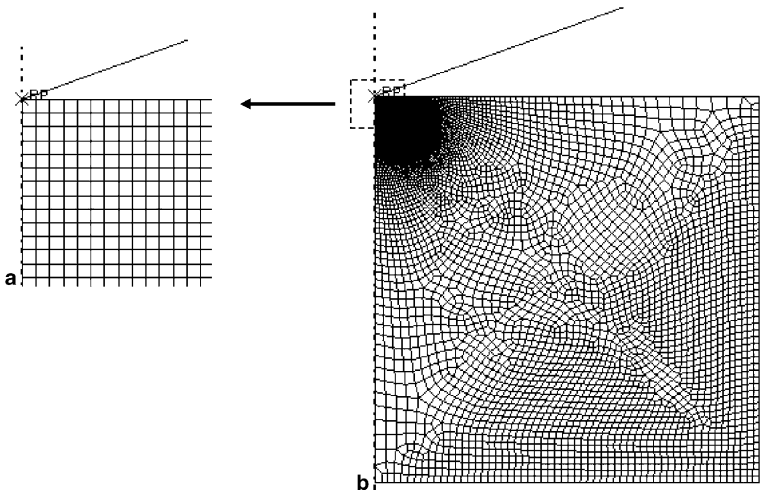

Fig. 1. Typical axisymmetric finite element mesh: (a) zoom-up of mesh near contact region and (b) mesh for target domain.

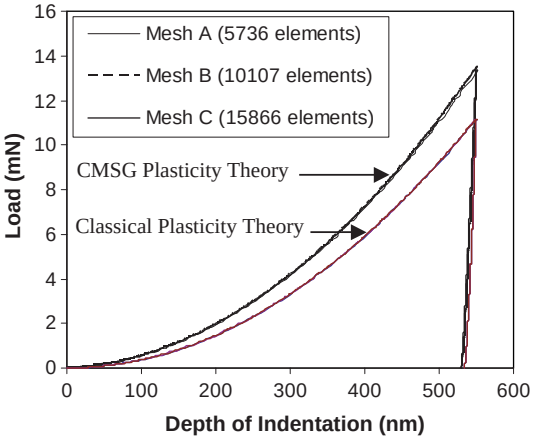

Fig. 2. Results of mesh convergence studies.

A series of C^0 solid elements incorporating plastic strain gradient effects was proposed by Swaddiwudhipong et al. (2005a). These solid elements are employed to simulate both Berkovich and equivalent conical indentation tests. The solutions obtained and those based on axisymmetric finite element with and without the strain gradient effects are depicted and compared with the experimental data reported by Pethica et al. (1983) in Fig. 3.

The comparison of these results demonstrates clearly the hardening effects of materials subject to indentation at micron and submicron levels. Numerical results obtained from the proposed finite element model incorporating CMSG plasticity theory agree reasonably well with indentation test results. In contrast, conventional finite element solutions deviate significantly from the test results conducted at submicron level.

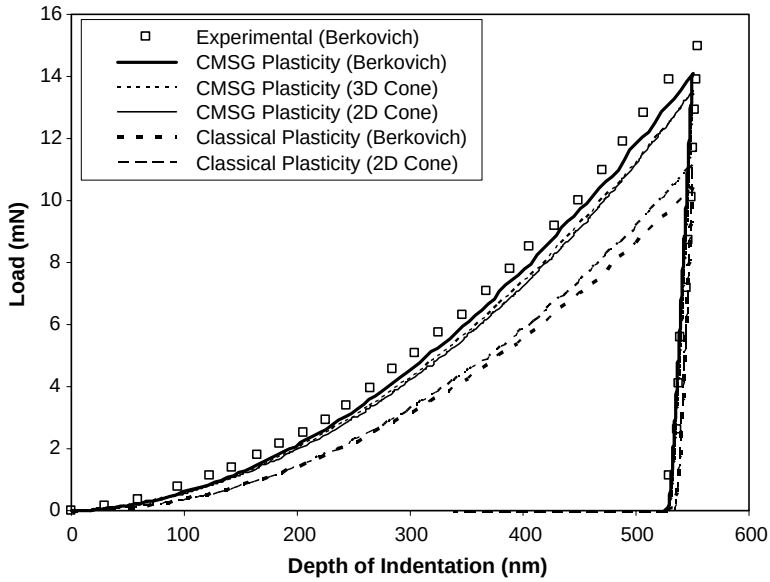

Fig. 3. Comparison of numerical and experimental results.

The numerical results obtained from the proposed axisymmetric finite element and those from solid elements are by and large identical.

It is interesting to note that the load–displacement curve of the Berkovich indenter lies below that of the conical indenter when conventional plasticity theory is adopted whereas the reversed trend is observed if the CMSG plasticity theory is included in the element formulation. This is despite the fact that the contact area to indentation depth relationship for both Berkovich and conical indenters is identical. The apparent contradiction of this observation is most likely due to the following phenomenon. In the conventional plasticity model, high level of stress concentration is induced in the region in the vicinity of apex and the edges of the Berkovich indenter initiating early localized yielding which reduces substantially the resistance to penetration of the indenter. For conical indenter, the localized yielding occurs early only at the tip of the indenter and further yielding, if any, on its cyclical smooth surface much later. For elements incorporating CMSG plasticity theory, the magnitude of plastic strain gradient in the region in the vicinity of the edges of the Berkovich indenter is large resulting in local stiffening effect whereas the gradient is substantially lower under the smooth surface of a conical indenter. It is observed that for nickel, the local material stiffening due to the strain gradient effect along the edges of the Berkovich indenter is larger than the weakening due to localized yielding due to stress concentration at the edges. Hence the force required by a Berkovich indenter is larger than that of a conical indenter to penetrate at the same depth of the target material. The phenomenon was also observed during the indentation tests conducted and reported earlier by Chollacoop et al. (2003).

The hardness of the Nickel materials in the present study is assessed by dividing the indentation load with the actual contact area taking into consideration the effect of sink-in and pile-up if any as suggested by Nix and Gao (1998). The variation of the hardness with respect to the indentation depth is depicted in Fig. 4. The hardness of the target materials is observed to increase significantly when the indentation depth decreases steadily at sub-micron level. This observation is consistent with analytical and experimental findings reported earlier by several researchers such as Nix and Gao (1998), Xu and Rowcliffe (2002) and Chen et al. (2004). The deformed configurations of the Nickel materials under simulated Berkovich indentation using both the classical plasticity and conventional mechanism-based strain gradient (CMSG) concept are displayed in Fig. 5. Pile-up is observed in the former. The phenomenon agrees well with the statement stipulated earlier by Xu and Rowcliffe (2002) that for materials with $n < 0.3$, pile-up is expected when the ratio

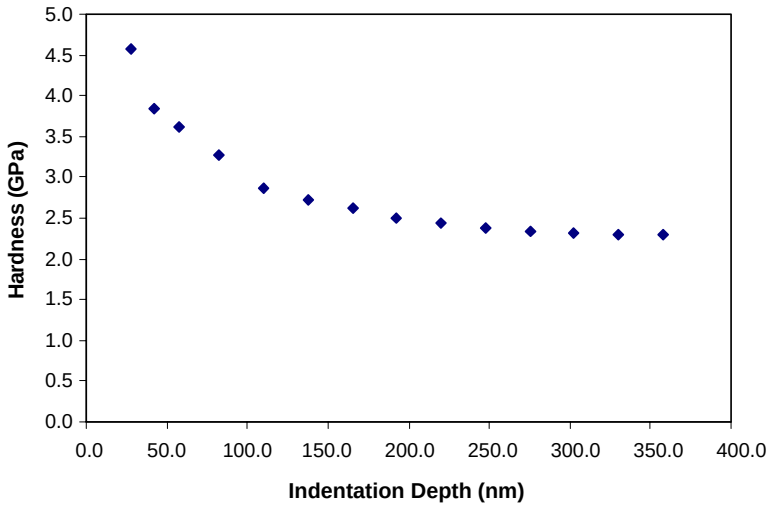

Fig. 4. Variation of hardness with indentation depth.

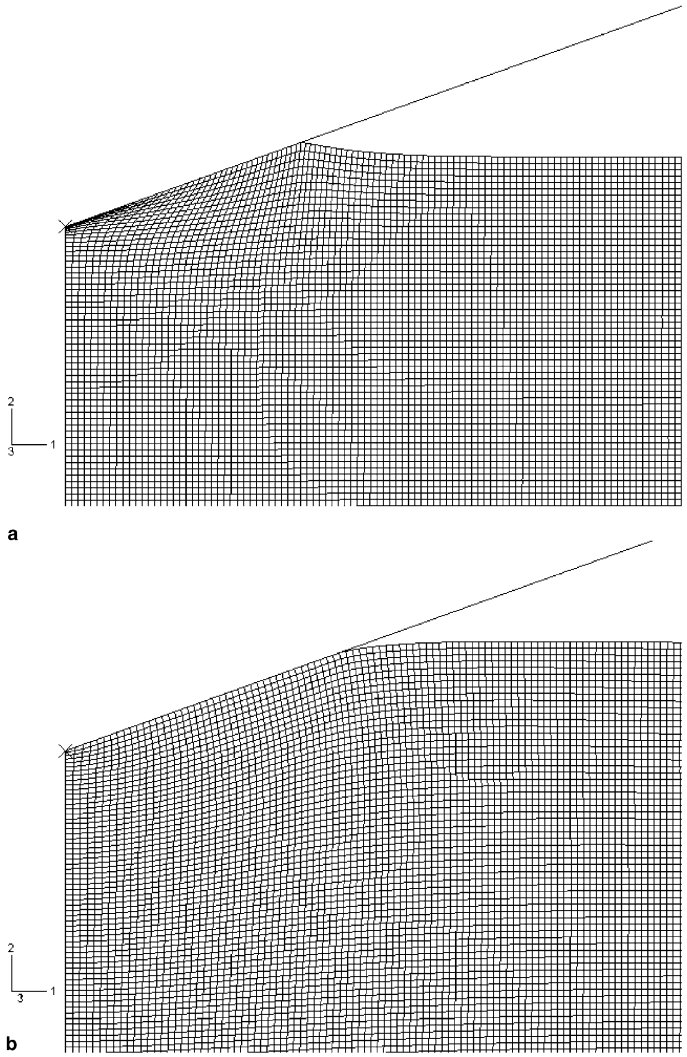

Fig. 5. Deformed shape of the mesh based on (a) classical plasticity model and (b) CMSG plasticity mode.

of the elastic recovered depth to the maximum penetration depth, $h_e/h_{max} < 0.12$. The values of n for Nickel and h_e/h_{max} obtained in the present study are 0.03 and 0.0297 respectively and hence it is not surprising that pile-up is observed. However, when the plastic strain gradient effect is included, a mild sink-in is noticed. This latter phenomenon is most likely attributed to the hardening of materials in the vicinity of the contact region where the effect of strain gradient plasticity is prominent.

6. Conclusions

C^0 axisymmetric finite element for materials with plastic strain gradient effects has been proposed in the present study. Conventional mechanism-based strain gradient plasticity is incorporated through the intrinsic material length scale. As only the constitutive condition is affected, higher order stress and hence higher

order continuity requirements and/or additional nodal parameters with mixed formulation are no longer necessary. The proposed axisymmetric element has been adopted in the simulation of the Berkovich indentation on an electro-polished nickel. Comparison of the results with those obtained from indentation tests demonstrates clearly that indentation at submicron level can only be simulated reasonably accurately only when the effects of plastic strain gradient are included in the formulation of these finite elements. Numerical example also shows that though Berkovich and equivalent conical indenters with the same depth to area relation are adopted, significant deviation on load–indentation curves is observed. It is noted that when the effect of plastic strain gradient is included in the analysis, the material is hardened under Berkovich indenter due to higher strain gradient as compared to conical tip. The phenomenon was earlier obtained by Chollacoop et al. (2003) in their indentation tests.

References

ABAQUS/Standard User's Manual Version 6.3, 2002. Hibbit, Karlsson and Sorensen Inc.

Acharya, A., Bassani, J.L., 1996. On non-local flow theories that preserve the classical structure of incremental boundary value problems. In: Micromechanics of Plasticity and Damage of Multiphase Materials, IUTAM Symposium, Paris, August 29–September 1.

Aifantis, E.C., 1984. On the microstructural origin of certain inelastic models. Journal of Engineering Materials and Technology—Transactions of the ASME 106, 326–330.

Arsenlis, A., Parks, D.M., 1999. Cystallographic aspects of geometrically-necessary and statistically-stored dislocation density. Acta Materialia 47, 1597–1611.

Ashby, M.F., 1970. The deformation of plastically non-homogeneous alloys. Philosophical Magazine 21, 399–424.

Begley, M.R., Hutchinson, J.W., 1998. The mechanics of size-dependent indentation. Journal of the Mechanics and Physics of Solids 46, 2049–2068.

Bhattacharya, A.K., Nix, W.D., 1988. Finite element simulations of indentation experiments. International Journal of Solids and Structures 24, 881–891.

Bishop, J.F.W., Hill, R., 1951. A theory of plastic distortion of a polycrystalline aggregate under combined stresses. Philosophical Magazine 42, 414–427.

Bucaille, J.L., Stauss, S., Felder, E., Michler, J., 2003. Determination of plastic properties of metals by instrumented indentation using different sharp indenters. Acta Materialia 51, 1663–1678.

Chen, S.H., Wang, T.C., 2000. A new hardening law for strain gradient plasticity. Acta Materialia 48, 3997–4005.

Chen, S.H., Wang, T.C., 2002a. A new deformation theory for strain gradient effects. International Journal of Plasticity 18, 971–995.

Chen, S.H., Wang, T.C., 2002b. Finite element solutions for plane strain mode I crack with strain gradient effects. International Journal of Solids and Structures 39, 1241–1257.

Chen, J., Yuan, H., 2002. A micro-mechanical damage model based on gradient plasticity. International Journal for Numerical Methods in Engineering 54, 399–420.

Chen, S.H., Tao, C.J., Wang, T.C., 2004. A study of micro-indentation with size effects. Acta Mechanica 167, 57–71.

Chollacoop, N., Dao, M., Suresh, S., 2003. Depth-sensing instrumented indentation with dual sharp indenters. Acta Materialia 51, 3713–3729.

Eringen, A.C.m, 1981. On nonlocal plasticity. International Journal of Engineering Science 19, 1461–1474.

Eringen, A.C.m, 1983. Theories of nonlocal plasticity. International Journal of Engineering Science 21, 741–751.

Fleck, N.A., Hutchinson, J.W., 1993. A phenomenological theory for strain gradient effects in plasticity. Journal of the Mechanics and Physics of Solids 41, 1825–1857.

Fleck, N.A., Hutchinson, J.W., 1997. Strain gradient plasticityAdvances in Applied Mechanics, vol. 33. Academic Press, pp. 295–361.

Fleck, N.A., Muller, G.M., Ashby, M.F., Hutchinson, J.W., 1994. Strain gradient plasticity, theory and experiment. Acta Metallurgica et Materialia 42, 475–487.

Gao, H., Huang, Y., 2001. Taylor-based nonlocal theory of plasticity. Int. J. Solids Struct. 38, 2615–2637.

Gao, H., Huang, Y., Nix, W.D., Hutchinson, J.W., 1999. Mechanism-based strain gradient plasticity—I. Theory. Journal of the Mechanics and Physics of Solids 47, 1239–1263.

Giannakopoulos, A.E., Larsson, P.L., 1997. Analysis of pyramid indentation of pressure-sensitive hard metals and ceramics. Mechanics of Materials 25, 1–35.

Haque, M.A., Saif, M.T.A., 2003. Strain gradient effect in nanoscale thin films. Acta Materialia 51, 3053–3061.

Huang, Y., Gao, H., Nix, W.D., Hutchinson, J.W., 2000. Mechanism-based strain gradient plasticity—II. Analysis. Journal of the Mechanics and Physics of Solids 48, 99–128.

Huang, Y., Qu, S., Hwang, K.C., Li, M., Gao, H., 2004. A conventional theory of mechanism-based strain gradient plasticity. International Journal of Plasticity 20, 753–782.

Hutchinson, J.W., 1976. Bounds and self-consistent estimates for creep of polycrystalline materials. Proceedings of the Royal Society of London A 348, 101–127.

Kok, S., Beaudoin, A.J., Tortorelli, D.A., 2002. A polycrystal plasticity model based on the mechanical threshold. International Journal of Plasticity 18, 715–741.

Larsson, P.L., Giannakopoulos, A.E., Soderlund, E, Rowcliffe, D.J., Vestergaard, R., 1996. Analysis of Berkovich indentation. International Journal of Solids and Structures 33, 221–248.

Ma, Q.J., Clarke, D.R., 1995. Size dependent hardness in silver single crystals. Journal of Materials Research 10, 853–863.

Mindlin, R.D., 1965. Second gradient of strain and surface tension in linear elasticity. International Journal of Solids and Structures 1, 417–438.

Muhlhaus, H.B., Aifantis, E.C., 1991. The influence of microstructure-induced gradients on the localization of deformation in viscoplastic materials. Acta Mechanica 89, 217–231.

Nix, W.D., 1997. Elastic and plastic properties of thin films on substrates: nanoindentation techniques. Materials Science and Engineering A 234, 37–44.

Nix, W.D., Gao, H., 1998. Indentation size effect in crystalline materials, a law for strain gradient plasticity. Journal of the Mechanics and Physics of Solids 46, 411–425.

Nye, J., 1953. Some geometrical relations in dislocated crystals. Acta Metallurgica et Materialia 1, 153–162.

Pethica, J.B., Hutchings, R., Oliver, W.C., 1983. Hardness measurement at penetration depths as small as 20 nm. Philosophical Magazine A 48, 593–606.

Shu, J.Y., Fleck, N.A., 1998. The prediction of a size effect in micro-indentation. International Journal of Solids and Structures 35, 1363–1383.

Shu, J.Y., King, W.E., Fleck, N.A., 1999. Finite elements for materials with strain gradient effects. International Journal for Numerical Methods in Engineering 44, 373–391.

Stelmashenko, N.A., Walls, A.G., Brown, L.M., Milman, Y.V., 1993. Microindentation on W and Mo oriented single crystals: an STM study. Acta Metallurgica et Materialia 41, 2855–2865.

Stolken, J.S., Evans, A.G., 1998. A microbend test method for measuring the plasticity length scale. Acta Materialia 46, 5109–5115.

Swaddiwudhipong, S., Hua, J., Tho, K.K., Liu, Z.S., 2005a. C^0 solid elements for materials with strain gradient effects. International Journal for Numerical Methods in Engineering (in press).

Swaddiwudhipong, S., Tho, K.K., Liu, Z.S., Zeng, K., 2005b. Material characterization based on dual indenters. International Journal of Solids and Structures 42, 69–83.

Taylor, G.I., 1934. The mechanism of plastic deformation of crystals. Part I—theoretical. Proceedings of the Royal Society of London A 145, 362–387.

Toupin, R.A., 1962. Elastic materials with couple stresses. Archive for Rational Mechanics and Analysis 11, 385–414.

Wang, W., Huang, Y., Hsia, K.J., Hu, K.X., Chandra, A., 2003. A study of microbend test by strain gradient plasticity. International Journal of Plasticity 19, 365–382.

Xia, Z.C., Hutchinson, J.W., 1996. Crack tip fields in strain gradient plasticity. Journal of the Mechanics and Physics of Solids 44, 1621–1648.

Xu, Z.H., Rowcliffe, D., 2002. Method to determine the plastic properties of bulk materials by nanoindentation. Philosophical Magazine A 82, 1893–1901.

Zienkiewicz, O.C., Taylor, R.L., 1994. The Finite Element Method. McGraw-Hill, New York.